JCI insight

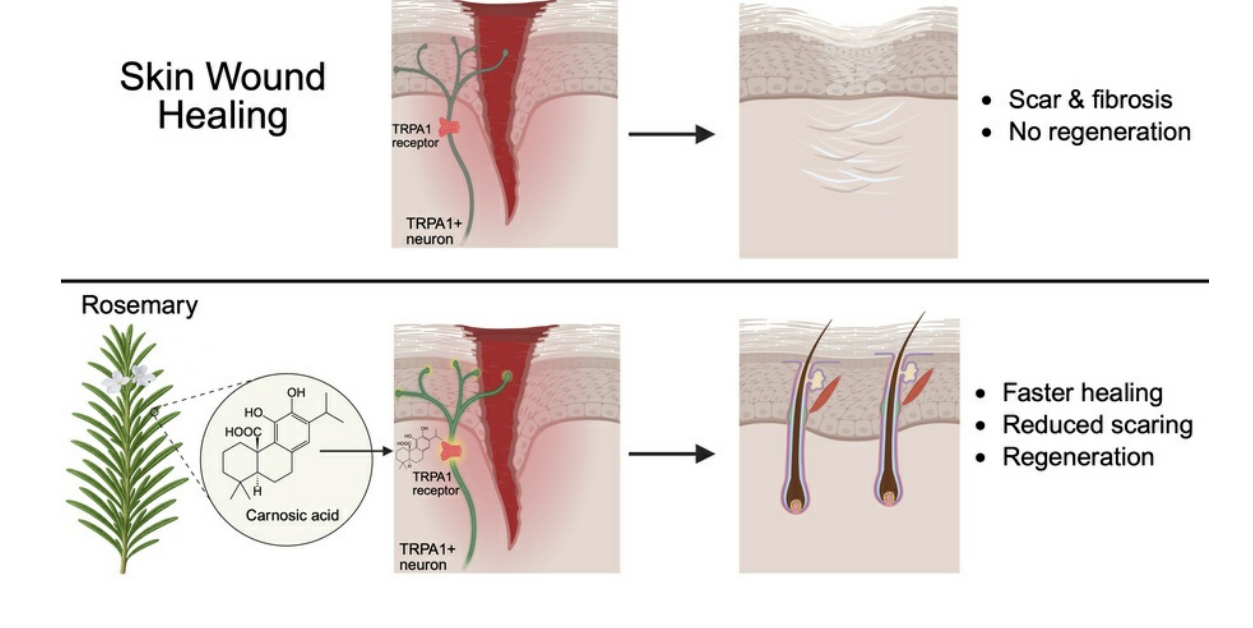
Carnosic acid in topical rosemary extract enhances skin repair via TRPA1 activation

Emmanuel Rapp, ..., Christopher A. Reilly, Thomas H. Leung

JCI Insight. 2025. https://doi.org/10.1172/jci.insight.196267.

Research In-Press Preview Dermatology Inflammation

Graphical abstract



Find the latest version:



1	Carnosic acid in topical rosemary extract enhances skin repair via TRPA1 activation
2	
3	Authors and Affiliations
4	Emmanuel Rapp ^{1*} , Jiayi Pang ^{1*} , Borna Saeednia ² , Stephen M. Prouty ¹ , Christopher A. Reilly ³ , Thomas H
5	Leung ^{1,4,#}
6	1. Department of Dermatology, University of Pennsylvania, Philadelphia, Pennsylvania, United
7	States of America.
8	2. Department of Chemistry, University of Pennsylvania, Philadelphia, Pennsylvania, United States
9	of America.
10	3. Department of Pharmacology and Toxicology, Center for Human Toxicology, University of Utah
11	Salt Lake City, Utah, United States of America.
12	4. Corporal Michael J. Crescenz Department of Veterans Affairs Medical Center, Philadelphia,
13	Pennsylvania, United States of America.
14	* These authors occupy the first position in the author byline equally.
15	# Correspondence:
16	Thomas Leung, MD, PhD
17	421 Curie Blvd, BRB 1039, Philadelphia PA 19104
18	thl@pennmedicine.upenn.edu
19	
20	Conflict-of-interest statement
21	The authors have declared that no conflict of interest exists.

Abstract (151)

Mammalian skin wounds typically heal with a scar, characterized by fibrotic tissue that disrupts original tissue architecture and function. Therapies that limit fibrosis and promote regenerative healing remain a major unmet clinical need. Rosemary extract, particularly in the form of topical oils and creams, has gained widespread public attention for its purported wound-healing properties. However, its efficacy and mechanism of action remain poorly understood. We show in adult wound healing mouse models that an ethanol-based rosemary extract accelerates the speed of wound healing and mitigates fibrosis.

Mechanistically, we identify that carnosic acid, a major bioactive component of rosemary leaves, activates the TRPA1 nociceptor on cutaneous sensory neurons to enhance tissue regeneration. Mice lacking TRPA1 in sensory neurons do not exhibit these pro-regenerative responses, confirming its role as a critical mediator. Together, these findings suggest that topical rosemary extract may represent an effective and accessible therapeutic approach to improve skin repair outcomes.

Introduction

Skin wounds affect 100 million patients per year in the United States, and these wounds may heal by two different biological processes: scar formation or tissue regeneration (1,2). Scars cause loss of original tissue architecture and function, while tissue regeneration reconstitutes the major components of the skin, such as hair follicles, sebaceous glands, and cartilage (3). Most human skin wounds heal with a fibrotic scar, which, depending on the location, may cause substantial functional morbidity. Methods to prevent scar formation or to promote scarless wound healing remain a major unmet clinical need (4).

Ear hole closure is a well-established mouse model of skin injury (5–8). Typically, 2 mm through-and-through holes in the mouse ear pinna of wild type (WT) C57BL/6J mice heal with a scar and remain open, similar to a human earring piercing. We and others have previously shown that some strains of mice may heal with tissue regeneration that results in the complete closure of ear holes, and the healed tissue exhibit return of original tissue architecture and decreased fibrosis. More specifically, we previously showed that activation of TRPA1 nociceptor by imiquimod (IMQ) or allyl isothiocyanate (AITC) promotes scarless wound healing (9). Activated TRPA1 stimulated local production of interleukin-23 (IL-23) by dermal dendritic cells, leading to activation of circulating dermal interleukin-17 (IL-17)- and interleukin-22 (IL-22)-producing γδ T cells, promoting full ear wound closure.

Herbs and plants have historically been used as successful disease treatments due to their medicinal properties, and approximately 25% of drugs prescribed worldwide are of plant origin (10, 11). Social media platforms, including TikTok, Instagram, and YouTube, have numerous videos describing the potential therapeutic effects of the *Rosmarinus officinalis* (rosemary) plant to reduce scar formation, promote hair growth, and improve facial skin health, with some of the most popular videos amassing over 20 million views (12–14). The rosemary-containing health care products market was valued at USD \$980.8 million in 2023 (15). Despite the widespread promulgation and belief about the medicinal

properties of rosemary, there is a lack of robust and rigorous scientific studies detailing its therapeutic effects.

We demonstrate that rosemary extract promotes scarless wound healing in mouse skin and identify carnosic acid as the active ingredient. We show that rosemary activates the TRPA1 receptor on sensory nerves to promote tissue regeneration.

Results

Rosemary promotes scarless wound healing

To test rosemary's role in wound healing, we purchased rosemary from the supermarket, physically minced their leaves, performed an ethanol extraction, and spatulated the mixture into a Cetaphil cream base. After performing a 2 mm through-and-through ear punch through the pinna of mouse ears, we applied rosemary or vehicle control cream on the ears daily for four weeks. Rosemary cream closed ear holes to a smaller size compared to vehicle control cream-treated ears (Figure 1A-B). Histological analysis of rosemary cream-treated mouse ear wounds exhibited increased return of normal tissue architecture, with regeneration of hair follicles, sebaceous glands, and subcutaneous fat. We also observed shortened distances between opposing cartilage end plates, supporting cartilage regeneration (Figure 1C-E). Mouse ears are a unique anatomic location, and we wanted to determine whether these observations were generalizable to other areas of skin. Stented dorsal back skin wounds on mice typically heal with scar formation but may also exhibit regenerative phenotypes (16). Stented 6 mm dorsal back skin wounds treated with rosemary cream displayed faster re-epithelialization than control mice (Figure 2A-B). This suggests that rosemary treatment can promote wound healing at other skin sites. Together, these data show that a cream containing ethanol-extracted rosemary leaves promotes mouse wound regeneration. Next, we wanted to identify the active ingredient.

Carnosic acid in rosemary leaves promotes regeneration

Although different rosemary-containing extracts have undergone mass spectrometry profiling, the chemical composition resulting from our ethanol-based extraction method remained unknown (17). We performed UPLC coupled with mass spectrometry on our ethanol-based rosemary extract. Consistent with prior studies, the two most abundant compounds were carnosic acid and carnosol, its oxidation product (Table 1) (18, 19). To directly test if carnosic acid may enhance wound healing, we compounded carnosic acid (5 mg/mL) into a Cetaphil cream base and performed our ear hole closure assay. After 4 weeks, carnosic acid cream treated ears closed to an average of ~90% of the original wound size compared to

~35% for vehicle control cream-treated ears (Figure 3A-B). Histological analysis of carnosic acid cream-treated mouse ear wounds stained with H&E revealed increased return of hair follicles, sebaceous glands, and subcutaneous fat. A shorter distance between the opposing cartilage end plates supported cartilage regeneration (Figure 3C-D). Finally, we measured fibrosis by picrosirius red stain. Ears treated with either rosemary or carnosic acid cream revealed significantly less fibrosis at the wound edge compared to vehicle control cream (Figure 3E-F). Taken together, carnosic acid is a key biologically active compound in the rosemary plant that promotes scarless wound healing. We believe its effectivessness and potency are similar to rosemary cream, with only the Week 2 time point being statistically significant between the two treatments.

Rosemary extract activates the TRPA1 ion channel

Prior work demonstrated that carnosic acid acts as a ligand for the transient receptor potential ankyrin 1 (TRPA1) receptor, and our lab showed that the activation of TRPA1 promotes full ear wound closure in mice (9, 20). To test if rosemary-induced ear wound closure was mediated by TRPA1, we screened whether rosemary and multiple other plant extracts may act as agonists of the TRPA1 channel. Compared to AITC as a positive control, we found that mint, oregano, fennel seed, nutmeg, thyme, allspice, and rosemary induced TRPA1 receptor-mediated calcium influx. (Figure 4A, S1). We next compared whether thyme and rosemary extracts activated other members of the TRP ion channel family. Both rosemary and thyme extracts specifically activated the TRPA1 ion channel, although rosemary modestly activated the TRPV3 channel (~15%) (Figure 4B). We noted that cilantro did not activate TRPA1 (Figure 4A), and cilantro has not been reported to generate carnosic acid (21–23). As a negative control, we compounded an ethanol-based cilantro extract into a Cetaphil cream base and repeated our ear hole assay. Cilantro cream did not result in increased ear hole closure compared to vehicle control creamtreated mouse ears (Figure 4C-D).

Based on our prior work, we showed that local activation of TRPA1 with IMQ or AITC improved wound healing on distal sites suggesting a systemic effect. We tested this possibility in two different

ways. 1) Wound induced hair neogenesis (WIHN) involves large excisional back wounds that may regenerate with new hair follicles (24). We performed WIHN on WT mice and rubbed rosemary cream or control cream on the ears of mice every day for 28 days. Compared to control mice, rosemary-treated mice did not exhibit more hair follicle regeneration (Figure S2A-S2B). 2) We rubbed control cream or rosemary cream on shaved dorsal back skin and performed our ear hole closure assay. We observed a minimal, not clinically relevant difference in ear hole closure between rosemary-treated mice and control mice (Figure S2C-S2D). We conclude that rosemary cream only enhances locally treated wound healing and does not function in a systemic manner.

126

127

128

129

130

131

132

133

134

135

136

137

138

139

140

141

142

143

118

119

120

121

122

123

124

125

Key TRPA1 pathway mediators are induced in rosemary-treated ear wounds.

To further verify the involvement of the TRPA1-mediated signaling pathway in rosemarymediated wound healing, we performed bulk RNA-sequencing on wound edge tissue from ears treated for one week with rosemary or vehicle control cream (Figure 5A-B). PCA analysis demonstrated that treatment groups segregated across the first principal component, indicating that the biggest source of variation is between treatment groups (Figure 5C). Rosemary cream induced the expression of IL-23a, IL-22, and IL-17a transcripts, all components previously demonstrated to be necessary for TRPA1-mediated wound healing (Figure 5D). Additionally, gene ontology biological processes analysis revealed upregulation of γδ T cell activation, IL-23-mediated signaling, and IL-17 production. The Enrichr pathway with the highest combined score was IL-23-mediated signaling (Figure 5E-F). Because of the observed decrease in fibrosis, we wanted to interrogate the pro-fibrotic myofibroblast response in rosemary-treated ears. We collected wound-edge tissue of control cream- or rosemary cream-treated ears at 1-week post-injury and assessed pro-fibrotic myofibroblast gene expression by qPCR. Compared to control cream, rosemary-treated ears exhibited 2-fold more Acta2 expression and 2-fold less Col3a1 expression (Figure S3). We saw no differences in Colla1, Fn1, and Vim levels (Figure S3). We conclude that rosemary-treated ears may still induce myofibroblast generation and activation, however the proregenerative pathway induced by TRPA1 may be more dominant than the fibrotic response. Taken

together, these gene expression changes are aligned with our prior work dissecting how activation TRPA1-receptor promotes scarless tissue regeneration.

Neuronal-specific TRPA1 deletion abrogated rosemary-induced wound healing

We and others have described that TRPA1 is mainly expressed in a subset of TRPV1-expressing neurons located in dorsal root ganglia (DRGs) (9, 25, 26). To test whether TRPA1-expressing neurons are necessary for rosemary-mediated tissue regeneration, we generated mice specifically lacking TRPA1 in sensory neurons (TRPA1^{fl/fl}:TRPV1^{Cre}, referred to as nTRPA1-KO). We previously demonstrated that daily application of topical IMQ promotes complete ear hole closure in WT mice (9). To confirm successful generation of nTRPA1-KO mice, we treated injured ears of nTRPA1-KO or WT littermate control mice with daily IMQ for four weeks. IMQ-treated WT mice closed their ear holes to a significantly smaller size compared to IMQ-treated nTRPA1-KO mice (~92% vs ~45%, respectively, Figure 6A). Notably, vehicle-treated nTRPA1-KO mice also exhibited ~45% ear hole closure. Thus, neuronal-specific TRPA1 is necessary for IMQ-induced tissue regeneration.

Next, we treated nTRPA1-KO mice with rosemary cream. We observed that rosemary cream-treated nTRPA1-KO mice closed their ear holes to a larger size compared to rosemary cream-treated WT control mice, thus exhibiting impaired tissue regeneration (Figure 6B-C). Thus, peripheral nerve expression of TRPA1 is necessary for rosemary-mediated skin regeneration.

Discussion

We demonstrate that topical rosemary extract enhances mammalian skin repair. Rosemary activates TRPA1+ sensory neurons to induce these effects, and carnosic acid within rosemary leaves acts as an active ingredient. Indeed, this work confirms that rosemary oils and cream, as reported on many social media sites, may reduce fibrosis and improve skin repair.

Plant extracts have long been used in traditional medicine, but oftentimes the active ingredient remains unknown or unidentifiable. We successfully identified that carnosic acid in rosemary leaves is a key biologically active component that promotes scarless tissue regeneration. Our plant screen also identified oregano and thyme as other plants that activate TRPA1, and prior work demonstrated that both plants generate carnosic acid or carnosol, an oxidation product of carnosic acid (27, 28). Both products are reported to activate TRPA1 (20). TRPA1 receptor activation is primarily triggered by electrophilic irritants such as AITC (mustard oil), cinnamaldehyde, or JT010. Future studies are needed to assess whether oxidation of carnosic acid to carnosol is necessary to promote scarless wound healing. We identified that mint, fennel, nutmeg, and allspice may also activate TRPA1. We speculate that these plants may also be compounded into a cream to promote wound healing. However, more work is needed to determine their active ingredient(s).

Rosemary extract exhibited minor activation of the TRPV3 receptor. We did not detect any notable TRPV3 agonists in our UPLC/MS analysis. Prior literature demonstrated that carnosol and carnosic acid do not activate TRPV3, and TRPV3 activation has not been reported to induce wound healing (20). Thus, we do not believe that TRVP3 activation is a contributing factor in our studies.

Human and mouse skin exhibit many differences, including resident immune cell populations. We previously showed that TRPA1-mediated tissue regeneration requires $\gamma\delta$ T cells, which may reside in the epidermis or dermis. While mice have more $\gamma\delta$ T cells in the epidermis (also known as dendritic

epidermal T cells) compared to humans, both mouse and human skin contain similar numbers of dermal $\gamma\delta$ T cells. Moreover, mouse and human dermal $\gamma\delta$ T cells were shown to promote wound healing via secreting insulin-like growth factor 1 and fibroblast growth factor 9 (29–32). We speculate that TRPA1-activation may promote tissue regeneration through either population of $\gamma\delta$ T cells, and rosemary-extract may induce scarless tissue regeneration in human skin. While CD4+ helper T cells have been reported to express TRPA1, they express TRPA1 by orders of magnitude lower was shown to not be a key regulator of T-cell receptor-stimulated calcium signaling (33). Additionally, the calcium influx of TRPA1 in these cells has not been reported to mediate wound healing. Taken together, we think that T cells contribute to the enhanced wound healing but it is not a direct effect via TRPA1 on T cells. Additional studies are needed to explore these possibilities.

While IMQ and AITC have proven effective to promote scarless wound healing, potential side effects have limited their use in regenerative medicine (34–36). IMQ was originally designed to activate the toll-like receptor 7 (TLR7) to promote inflammation and innate immunity and its ability to activate TRPA1 was a non-specific side-effect. AITC is the gold-standard TRPA1 agonist and is a well-established caustic chemical that may cause severe chemical-induced irritation or burns to tissues. Our rosemary extract is substantially less caustic than AITC. Moreover, carnosic acid has not been reported to activate the TLR7 pathway or to possess corrosive or tissue-damaging properties. In fact, carnosic acid may attenuate allergic inflammatory mediators in activated mast cells and function as an antioxidant (27, 37, 38). Carnosic acid is typically localized within the chloroplasts, the organelles in plant leaves responsible for photosynthesis. It acts as a free radical scavenger and neutralizes harmful reactive oxygen species generated during photosynthesis (27, 39). Being less caustic may come at a cost. Our prior work showed that activation of TRPA1 could induce a systemic wound healing effect. We observed that activation of TRPA1 by rosemary did not induce a systemic wound healing effect. We believe this may be related to the concentration of agonist in these experiments. Rosemary cream was approximately 40% as effective as AITC in our in vitro experiments (Figure 4). This difference may also explain why AITC is

more caustic than rosemary cream. Further studies will be needed to determine optimal concentrations of rosemary for local and systemic wound healing effects. Taken together, rosemary extract or carnosic acid may represent an ideal TRPA1-agonist to promote local scarless tissue regeneration.

These results demonstrate that the enthusiasm publicized on social media may be correct, and rosemary-containing extracts reduce mammalian skin scar formation. These results coupled with the widespread accessibility of the rosemary plant and its relatively low cost should motivate formal testing of rosemary-containing creams to reduce scar formation in human clinical trials.

Methods

Sex as a biological variable. This wound healing study examined male and female animals; similar findings are reported for both sexes. Further studies are needed to assess whether the rosemary plant can display sex-specific effects.

Animal models. C57BL/6J (strain #000664), 129S-*Trpa1*^{tm2Kykw}/J (TRPA1^{fl/fl}, strain #008649), and B6.129-*Trpv1*^{tm1(cre)Bbm}/J (TRPV1^{Cre}, strain #017769) mice were obtained from The Jackson laboratory. TRPA1^{fl/fl} mice were crossed with TRPV1^{Cre} mice to obtain mice deficient for TRPA1 specifically in TRPV1-expressing neuronal cells. All mouse genotypes were verified by standard PCR as described by the Jackson Laboratory (protocols 28644 and 35042). Mice were housed at the University of Pennsylvania animal care facilities on a 12-hour light/12-hour dark cycle with free access to normal chow and water. All mice were used between 6-8 weeks of age.

Animal injury. For ear wounding, we used a standard 2mm mechanical punch (Roboz) to create a through-and-through hole in the center of each outer ear (pinna). We applied ~50 mg of treatment cream to injured mouse ears every day for one month. Ear hole diameter of wound edge tissue was measured using a dissection microscope (Nikon) in the horizontal and vertical directions on a weekly basis. Preestablished criteria required the exclusion of ears if there were signs of wound infection, tearing of the ear, or abnormal geometric shape. No points were excluded in this study. For wound induced hair neogenesis, 1.5-cm² full-thickness skin wounds were made as previously described (24). We applied ~50 mg of treatment cream adjacent to the wounded area every day for 4 weeks. After 4 weeks, de novo hair follicles were identified by whole-mount alkaline phosphatase staining of dermis preparations as previously described (24). For stented back wounds, a 6mm disposable biopsy punch (Acuderm) was used to make two circular full thickness wounds on the dorsal back skin of mice. Silicon wound splints (Grace Bio-Labs) were sutured with 4-0 Nylon to prevent skin contracture. We applied ~50 mg of

treatment cream around the stented wound every day for 4 weeks. Re-epithelialized skin borders were used to measure percent wound closure.

Injury Treatments. To generate the rosemary and cilantro creams, dried rosemary or cilantro extract was resuspended in 500 μL of DMSO. Cetaphil cream was added to obtain a final concentration of 12 mg of rosemary or cilantro extract/mL. Carnosic acid cream was generated by resuspending 50 mg of carnosic acid (Santa Cruz Biotechnology, sc-202520A) in 250 μL DMSO. Cetaphil cream was added to obtain a final concentration of 5 mg/mL. Vehicle control cream for each treatment was generated by adding an equal volume of treatment vehicle to Cetaphil cream. Imiquimod cream USP 5% (12.5 mg/0.25 g, NDC 68462-536-70) was obtained from Glenmark Pharmaceuticals, NJ.

Plant extractions. Fresh rosemary or cilantro plant leaves (Trader Joe's, 1324 Arch St, Philadelphia, PA 19107) were weighed (~15 g) and minced in the presence of ethanol (~30 mL) in a 50 mL conical. The minced leaves in ethanol were stored overnight at -80° C. The minced leaves were then discarded, and the liquid solution was filtered through a 0.22 μm vacuum filtration system (03359, Sigma). The ethanol in the solution was evaporated under vacuum in a 37° C water bath to obtain the dried rosemary or cilantro extract. For TRP calcium flux assays, fresh herb/plant leaves or spices (200 mg) were minced in DMSO and extracted overnight at 4°C, clarified by centrifugation, and stored at -20°C. The DMSO extract was diluted to 0.25 mg/mL in LHC9 for calcium flux assays.

UPLC-MS Analysis. Chromatographic separation was performed on a Waters Acquity ultra performance liquid chromatography (UPLC) I-Class Plus Instrument (Milford, MA) equipped with a binary gradient pump and TUV two channel UV detector. A Waters (Milford, MA) Acquity UPLC HSS C18 column (2.1 x 50 mm, 1.8 μm particle size), along with a prefilter, was used with the column temperature maintained at 30 °C. A binary eluent system was employed with mobile phase A (water with 0.1% formic acid) and mobile phase B (acetonitrile with 0.1% formic acid) with a flow rate of 0.5 mL/min and a gradient

274 program as follows: 0.00-0.50 min, 5% B; 0.50-12.50 min, linear from 5% to 95% B; 12.50-14.50 min, 275 95% B; 14.50-15.00 min, 5% B. For the preparation of the eluents, Optima™ LC/MS-grade water, 276 acetonitrile, and formic acid were purchased from Fisher Scientific and used without further purification. 277 The sample injection volume was 2 µL. The UV detector was set to 254 nm. 278 The UPLC instrument was coupled to a Waters SQD2 single quadrupole mass spectrometer (Milford, MA) 279 with a Zspray electrospray ionization source using nitrogen as desolvation and nebulization gas. Source 280 conditions were as follows: capillary voltage, 1.50 kV; cone voltage, 30 V; desolvation temperature, 600 281 °C; desolvation gas flow rate, 1000 L/h; cone gas flow rate, 0 L/h. The mass spectrometer was operated in 282 negative ESI-mode scanning m/z 50-1000. 283 284 TRP channel overexpression: Human TRPA1, V1, V2, V3, V4, and M8 genes were subcloned into the 285 pcDNA 3.1D-V5/His6 mammalian expression vector (Invitrogen), as previously described (40–42). 286 Individual plasmids were transfected into HEK-293 cells (ATCC) which exhibit minimal/absent basal 287 response to the TRP channel agonists. Stable lines were selected by using Geneticin (400 µg/mL) 288 (Invitrogen) and isolating homogeneous colonies by dilution. TRPM2-overexpressing HEK-293 cells 289 were provided by Dr. Yasuo Mori (Kyoto University, Kyoto, Japan) and generated as previously 290 described (43, 44). All overexpressing cells were maintained in DMEM/F12 supplemented with 5% FBS, 291 1X anti/anti and 300 μg/mL Geneticin. 292 293 TRP Screening Assays/Calcium Influx Assays. Calcium flux assays were performed as previously 294 described (45). Briefly, HEK-293 cells stably overexpressing TRPA1, TRPM2, TRPM8, TRPV1, 295 TRPV2, TRPV3, or TRPV4 were used. Changes in fluorescence intensity indicative of an increase in 296 intracellular calcium were measured using the Fluo-4 Direct assay kit (F10472, Thermo Fisher) on a 297 BMG Labtech NOVOStar fluorescence plate reader. TRP-overexpressing HEK cells were plated in flat-298 bottom 96-well plates coated with 1% gelatin at ~30,000 cells/well and assayed at 90% confluence 1–2 d 299 post-plating. Prior to the assay, the cells were loaded with 1X Fluo-4 diluted 1:1 in LHC-9 (12680013,

Gibco) at 37 °C for 1 h. The Fluo-4 was removed, and the cells were washed with LHC-9 containing 1 mM probenecid (P36400, Thermo Fisher) and 0.75 mM trypan red (2456, ATT Bioquest). The assays were performed at 37 °C. Plant extract treatments (0.25 mg/mL in DMSO) were added to cells at 3X the desired final concentration in LHC-9 (111.1 μ M calcium). Reported values were corrected by subtracting the fluorescence response to a negative media control (i.e., no agonist) containing the appropriate concentrations of DMSO to match the extract samples. The data were further corrected by subtracting the fluorescence response of HEK-293 cells lacking TRP expression with the data reported as the percent of response relative to each TRP channel's respective specific agonist (positive control): TRPA1 = 250 mM AITC, TRPM2 = 1mM H₂O₂, TRPM8 = 50 mM icilin, TRPV1 = 1 mM nonivamide, TRPV2 = 250 mM D⁹-tetrahydrocannbinol, TRPV3 = 250 mM carvacrol, or TRPV4 = 35 nM GSK 1016790A.

Histology. Standard histology and immunostaining protocols were followed, and investigators were blinded to tissue origin during histologic staining. In brief, the fresh skin tissue was fixed overnight at 4°C in 4% paraformaldehyde (J19943-K2, Thermo Fisher Scientific). The tissue was dried in 70% ethanol, trimmed, placed into tissue cassettes, processed (VIP5b, Sakura), and embedded into wax (Leica Paraplast X-tra) blocks. Blocks were cut using disposable blades (D554P, Sturkey) on a rotary microtome (RM2235, Leica) set at 5 μm thickness. Sections were floated on a water bath (145702, Boekel) set at 43°C and collected onto positively charged glass slides (Fisherbrand Superfrost Plus). Following overnight drying at room temperature, slides were baked for 30 minutes at 60°C, followed by H&E staining using an automated stainer (Leica Autostainer XL). Tissue embedding, sectioning, staining, and slide processing were performed in the Skin Biology and Disease Resource–Based Core (SBDRC) at the Department of Dermatology, University of Pennsylvania. H&E-stained sections were examined under bright-field microscopy and images acquired on a Keyence BZ-X700 microscope.

Picrosirius red (PSR) staining. The paraffin sections were dewaxed, hydrated, and the nuclei were stained with hematoxylin. Picrosirius red (Polysciences Inc., NC9908782) was added for one hour. The slides

were washed twice with acidified water (0.05% glacial acetic acid). The slides underwent dehydration in three changes of 100% ethanol, followed by clearing in xylene, and finally, mounting in a resinous medium. The PSR images were acquired on a Leica DM6B-Z microscope using a light polarizer equipped with a 32 mm quarter-wave plate and an ICT/P analyzer module. The acquired images were analyzed for fibrosis by quantifying the percent of collagen 1 (PSR) signal within the wounded tissue region using FIJI. Representative images were selected for figure panels. RNA isolation. A 6mm circular biopsy punch was used to capture the tissue surrounding the 2mm ear wound. The peripheral wound tissue from vehicle control cream treated- and rosemary cream-treated mouse ear wounds was homogenized using a Tissue-Tearor (985370, BioSpec Products), and RNA was isolated using an RNeasy kit (74106, QIAGEN). Real-time RT-PCR. Total RNA was quantified by UV absorbance on a Nanodrop (ThermoFisher) and complementary DNA (cDNA) (2 µg) was synthesized using the QuantiTect Reverse Transcription Kit (205313, Qiagen). The cDNA was then subjected to analysis by quantitative real-time PCR (qPCR) using TaqMan Fast Gene Expression Master Mix (ThermoFisher) and a Life Technologies QuantStudio 7 Pro instrument. The following TaqMan probe-based assays were used: Actb (Mm02619580 g1), Acta2 (Mm00725412 s1), Vim (Mm01333430 m1), Col1a1 (Mm00801666 g1), Col3a1 (Mm00802300 m1), Fn1 (Mm01256744 m1. mRNA expression was normalized to Actb and reported as relative expression using the comparative $\Delta\Delta$ Ct method. Bulk RNA library preparation. The RNA-seq libraries were made using the NEBNext Ultra II DNA Library Prep Kit for Illumina (E7760S, New England Biolabs) and NEBNext Multiplex Oligos for Illumina (E6609S, New England Biolabs) following the manufacturer's instructions and sequenced using

326

327

328

329

330

331

332

333

334

335

336

337

338

339

340

341

342

343

344

345

346

347

348

349

350

351

2 × 100-bp paired-end runs on Illumina HiSeq 2000/HiSeq 2500 platforms at BGI Americas.

Bulk RNA-seq analysis. Fastq files were aligned to the GRCm39 reference genome using STAR_2.4.0 in basic 2-pass mode using the Encode options as specified in the manual. Resulting BAM files were turned into a count matrix using the featureCounts program. Normalization by fragments per kilobase per million mapped fragments (FPKM) counts and differentially expressed transcripts were generated using the R packages edgeR and Limma, respectively.

Statistics. For in vivo time courses comparing hole size, data were analyzed using 2-way analysis of variance (ANOVA) using a temporal main effect, a main effect comparing treatment, and an interaction of the two main effects. For tests such that the two-way ANOVA indicates significant time-treatment interactions, an additional 2-tailed Student's t test was used, with p-values of less than 0.05 considered significant. For all other analyses, comparisons between two groups were carried out using a two-tailed unpaired Student's t-test unless otherwise indicated in the figure legend. In all tests, a p-value of less than 0.05 is considered significant. Levels of significance are indicated by the following: *p < 0.05, **p < 0.01, ***p < 0.001, and ****p < 0.0001 in the text.

Study approval. Experiments involving mice were reviewed and approved by the Institutional Animal Care and Use Committee of the University of Pennsylvania (protocol #805620). Mice were treated in accordance with the NIH guidelines for the humane care of animals.

371 Data availability.

The raw RNA sequencing data files can be accessed with GO accession number GSE298490 at https://www.ncbi.nlm.nih.gov/geo/query/acc.cgi?acc=GSE298490. This paper does not report any original code. Any additional information required to reanalyze the data reported in this paper is available from the lead contact upon request.

The supporting data values file is provided in the supplemental material.

378 **Author contributions:** 379 Experiment conceptualization, methodology and investigation performed by: E.R., J.P., B.S., S.P., C.R., 380 and T.L. 381 Bioinformatics analysis performed by: E.R. and J.P. 382 Writing of the manuscript performed by: E.R., J.P., and T.L. 383 Reviewing and editing the manuscript performed by: C.R. and T.L. 384 The order of authors in the first position of the author byline was determined by prioritizing manuscript 385 writing contribution. These criteria were pre-established and agreed upon by all authors. 386 387 **Acknowledgments:** 388 We thank Steve Prouty and the Penn Skin Biology Disease Resource Center (SBDRC) for their support. 389 T.H.L. receives support from Berstein Family, NIH (R01AR079483), VA (I01RX002701), Edwin and 390 Fanny Gray Hall Center for Human Appearance, and H.T. Leung Foundation.

391

392 References

- Sun BK, Siprashvili Z, Khavari PA. Advances in skin grafting and treatment of cutaneous wounds.
 Science. 2014;346(6212):941-945.
- 395 2. Marshall CD, et al. Cutaneous Scarring: Basic Science, Current Treatments, and Future Directions. 396 Adv Wound Care. 2018;7(2):29-45. doi:10.1089/wound.2016.0696
- 397 3. Takeo M, Lee W, Ito M. Wound Healing and Skin Regeneration. *Cold Spring Harb Perspect Med.* 2015;5(1):a023267. doi:10.1101/cshperspect.a023267
- 4. Sen CK, et al. Human Skin Wounds: A Major and Snowballing Threat to Public Health and the Economy. *Wound Repair Regen Off Publ Wound Heal Soc Eur Tissue Repair Soc*. 2009;17(6):763-771. doi:10.1111/j.1524-475X.2009.00543.x
- 5. Bedelbaeva K, et al. Lack of p21 expression links cell cycle control and appendage regeneration in mice. *Proc Natl Acad Sci U S A*. 2010;107(13):5845-5850. doi:10.1073/pnas.1000830107
- 404 6. Seifert AW, et al. Skin shedding and tissue regeneration in African spiny mice (Acomys). *Nature*. 405 2012;489(7417):561-565. doi:10.1038/nature11499
- 406 7. Leung TH, et al. A cellular, molecular, and pharmacological basis for appendage regeneration in mice. *Genes Dev.* 2015;29(20):2097-2107. doi:10.1101/gad.267724.115
- Huang J, et al. Granulocyte colony stimulating factor promotes scarless tissue regeneration. *Cell Rep.* 2024;43(10). doi:10.1016/j.celrep.2024.114742
- Wei JJ, et al. Activation of TRPA1 Nociceptor Promotes Systemic Adult Mammalian Skin
 Regeneration. *Sci Immunol*. 2020;5(50):eaba5683. doi:10.1126/sciimmunol.aba5683
- 412 10. Schmidt B, et al. A natural history of botanical therapeutics. *Metabolism*. 2008;57(7 Suppl 1):S3-S9. doi:10.1016/j.metabol.2008.03.001
- 414 11. Wachtel-Galor S, Benzie IFF. Herbal Medicine: An Introduction to Its History, Usage, Regulation,
- Current Trends, and Research Needs. In: Benzie IFF, Wachtel-Galor S, eds. *Herbal Medicine*:
- Biomolecular and Clinical Aspects. 2nd ed. CRC Press/Taylor & Francis; 2011. Accessed May 15,
- 417 2025. http://www.ncbi.nlm.nih.gov/books/NBK92773/
- 418 12. De Oliveira JR, Camargo SEA, De Oliveira LD. Rosmarinus officinalis L. (rosemary) as therapeutic and prophylactic agent. *J Biomed Sci.* 2019;26(1):5. doi:10.1186/s12929-019-0499-8
- 420 13. de Macedo LM, et al. Rosemary (Rosmarinus officinalis L., syn Salvia rosmarinus Spenn.) and Its Topical Applications: A Review. *Plants*. 2020;9(5):651. doi:10.3390/plants9050651
- 422 14. Ghasemzadeh Rahbardar M, Hosseinzadeh H. Therapeutic effects of rosemary (Rosmarinus
- 423 officinalis L.) and its active constituents on nervous system disorders. *Iran J Basic Med Sci.*
- 424 2020;23(9):1100-1112. doi:10.22038/ijbms.2020.45269.10541
- 425 15. Rosemary Hair Care Products Market Size Report, 2030. Accessed May 15, 2025.
- https://www.grandviewresearch.com/industry-analysis/rosemary-hair-care-products-market-report

- 427 16. Mascharak S, et al. Multi-omic analysis reveals divergent molecular events in scarring and
- regenerative wound healing. Cell Stem Cell. 2022;29(2):315-327.e6.
- 429 doi:10.1016/j.stem.2021.12.011
- 430 17. Sharma Y, et al. Full-Spectrum Analysis of Bioactive Compounds in Rosemary (Rosmarinus
- officinalis L.) as Influenced by Different Extraction Methods. *Molecules*. 2020;25(20):4599.
- 432 doi:10.3390/molecules25204599
- 433 18. Birtić S, et al. Carnosic acid. *Phytochemistry*. 2015;115:9-19. doi:10.1016/j.phytochem.2014.12.026
- 434 19. Loussouarn M, et al. Carnosic Acid and Carnosol, Two Major Antioxidants of Rosemary, Act
- through Different Mechanisms1[OPEN]. Plant Physiol. 2017;175(3):1381-1394.
- 436 doi:10.1104/pp.17.01183
- 20. Zhai C, et al. Identification of Natural Compound Carnosol as a Novel TRPA1 Receptor Agonist.
- 438 *Molecules*. 2014;19(11):18733-18746. doi:10.3390/molecules191118733
- 439 21. Msaada K, et al. Antioxidant activity of methanolic extracts from three coriander (*Coriandrum*
- 440 sativum L.) fruit varieties. Arab J Chem. 2017;10:S3176-S3183. doi:10.1016/j.arabjc.2013.12.011
- 441 22. Mechchate H, et al. Antioxidant, Anti-Inflammatory and Antidiabetic Proprieties of LC-MS/MS
- Identified Polyphenols from Coriander Seeds. *Molecules*. 2021;26(2):487.
- 443 doi:10.3390/molecules26020487
- 444 23. Sobhani Z, et al. Ethnobotanical and phytochemical aspects of the edible herb Coriandrum sativum
- 445 L. J Food Sci. 2022;87(4):1386-1422. doi:10.1111/1750-3841.16085
- 446 24. Ito M, et al. Wnt-dependent de novo hair follicle regeneration in adult mouse skin after wounding.
- *Nature*. 2007;447(7142):316-320. doi:10.1038/nature05766
- 448 25. Meng J, et al. TNFα induces co-trafficking of TRPV1/TRPA1 in VAMP1-containing vesicles to the
- plasmalemma via Munc18–1/syntaxin1/SNAP-25 mediated fusion. *Sci Rep.* 2016;6(1):21226.
- 450 doi:10.1038/srep21226
- 451 26. Yao K, et al. Inflammation—the role of TRPA1 channel. Front Physiol. 2023;14.
- 452 doi:10.3389/fphys.2023.1093925
- 453 27. Loussouarn M, et al. Carnosic Acid and Carnosol, Two Major Antioxidants of Rosemary, Act
- through Different Mechanisms1[OPEN]. *Plant Physiol*. 2017;175(3):1381-1394.
- 455 doi:10.1104/pp.17.01183
- 456 28. Nieto G, Ros G, Castillo J. Antioxidant and Antimicrobial Properties of Rosemary (Rosmarinus
- 457 officinalis, L.): A Review. *Medicines*. 2018;5(3):98. doi:10.3390/medicines5030098
- 458 29. Toulon A, et al. A role for human skin–resident T cells in wound healing. *J Exp Med*.
- 459 2009;206(4):743-750. doi:10.1084/jem.20081787
- 460 30. Pang DJ, et al. Understanding the complexity of γδ T-cell subsets in mouse and human.
- 461 *Immunology*. 2012;136(3):283-290. doi:10.1111/j.1365-2567.2012.03582.x

- 462 31. Hu W, et al. Skin γδ T Cells and Their Function in Wound Healing. Front Immunol. 2022;13.
- 463 doi:10.3389/fimmu.2022.875076
- 464 32. Zhang W, Pajulas A, Kaplan MH. γδ T cells in Skin Inflammation. *Crit Rev Immunol*.
- 465 2022;42(5):43-56. doi:10.1615/CritRevImmunol.2022047288
- 466 33. Szabó K, et al. TRPA1 Covalent Ligand JT010 Modifies T Lymphocyte Activation. *Biomolecules*.
- 467 2024;14(6):632. doi:10.3390/biom14060632
- 468 34. Allyl Isothiocyanate. In: Some Chemicals That Cause Tumours of the Kidney or Urinary Bladder in
- 469 Rodents and Some Other Substances. International Agency for Research on Cancer; 1999. Accessed
- 470 May 20, 2025. https://www.ncbi.nlm.nih.gov/books/NBK402129/
- 471 35. Andersen HH, et al. Dose–response study of topical allyl isothiocyanate (mustard oil) as a human
- surrogate model of pain, hyperalgesia, and neurogenic inflammation. *PAIN*. 2017;158(9):1723.
- 473 doi:10.1097/j.pain.0000000000000979
- 474 36. Elia MD, et al. Periocular Melanoma In Situ Treated With Imiquimod. *Ophthal Plast Reconstr Surg*.
- 475 2016;32(5):371. doi:10.1097/IOP.000000000000554
- 476 37. Crozier RWE, et al. Carnosic acid inhibits secretion of allergic inflammatory mediators in IgE-
- activated mast cells via direct regulation of Syk activation. *J Biol Chem.* 2023;299(4).
- 478 doi:10.1016/j.jbc.2022.102867
- 38. Satoh T, et al. Carnosic acid, a catechol-type electrophilic compound, protects neurons both in vitro
- and in vivo through activation of the Keap1/Nrf2 pathway via S-alkylation of targeted cysteines on
- 481 Keap1. J Neurochem. 2008;104(4):1116-1131. doi:10.1111/j.1471-4159.2007.05039.x
- 482 39. Munné-Bosch S, Alegre L. Subcellular Compartmentation of the Diterpene Carnosic Acid and Its
- Derivatives in the Leaves of Rosemary. *Plant Physiol.* 2001;125(2):1094-1102.
- 484 doi:10.1104/pp.125.2.1094
- 485 40. Reilly CA, et al. Capsaicinoids Cause Inflammation and Epithelial Cell Death through Activation of
- 486 Vanilloid Receptors. *Toxicol Sci.* 2003;73(1):170-181. doi:10.1093/toxsci/kfg044
- 487 41. Deering-Rice CE, et al. Electrophilic Components of Diesel Exhaust Particles (DEP) Activate
- 488 Transient Receptor Potential Ankyrin-1 (TRPA1): A Probable Mechanism of Acute Pulmonary
- 489 Toxicity for DEP. Chem Res Toxicol. 2011;24(6):950-959. doi:10.1021/tx200123z
- 490 42. Deering-Rice CE, et al. Transient Receptor Potential Vanilloid-1 (TRPV1) Is a Mediator of Lung
- Toxicity for Coal Fly Ash Particulate Material. *Mol Pharmacol*. 2012;81(3):411-419.
- 492 doi:10.1124/mol.111.076067
- 493 43. Shimizu S, et al. Inhibitory effects of AG490 on H2O2-induced TRPM2-mediated Ca2+ entry. Eur
- 494 *J Pharmacol.* 2014;742:22-30. doi:10.1016/j.ejphar.2014.08.023
- 495 44. Zong P, et al. TRPM2 enhances ischemic excitotoxicity by associating with PKCγ. Cell Rep.
- 496 2024;43(2):113722. doi:10.1016/j.celrep.2024.113722

497 45. Rapp E, et al. Mechanisms and Consequences of Variable TRPA1 Expression by Airway Epithelial Cells: Effects of TRPV1 Genotype and Environmental Agonists on Cellular Responses to Pollutants in Vitro and Asthma. *Environ Health Perspect*. 2023;131(2):027009. doi:10.1289/EHP11076

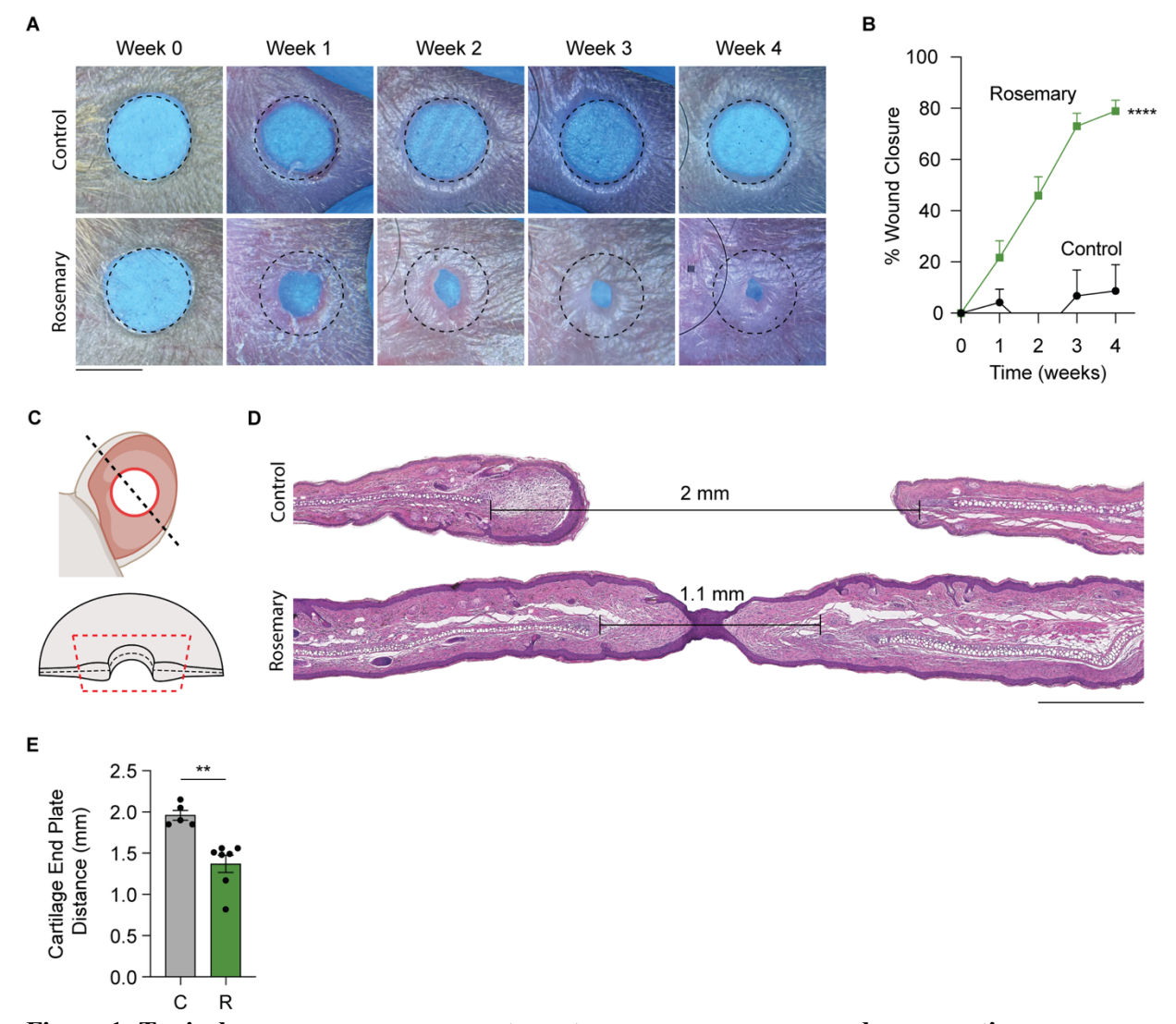


Figure 1: Topical rosemary cream promotes cutaneous mouse ear wound regeneration.

(A) Representative photographs of vehicle control cream- and rosemary cream-treated WT ears. Dotted circle represents original 2 mm hole-punch size. Black scale bar represents 2 mm. (B) Percentage of wound closure in vehicle control cream- (solid black line, n=7) and rosemary cream-treated (solid green line, n=12) WT mouse ears. Two-way ANOVA. (C) Schematic of mouse ear histology. (D) H&E-stained representative tissue sections from control- and rosemary cream-treated WT mouse ears. Distance between opposing cartilage endplates are indicated. Black scale bar represents 0.5 cm. (E) Bar plot quantifying cartilage endplate distance between vehicle control cream- and rosemary cream-treated WT mouse ears (C = control, R = rosemary). Student's t-test two tailed and unpaired. Data are presented as mean ± SEM. *P<0.05, **P<0.01, ***P<0.001, ****P<0.0001.

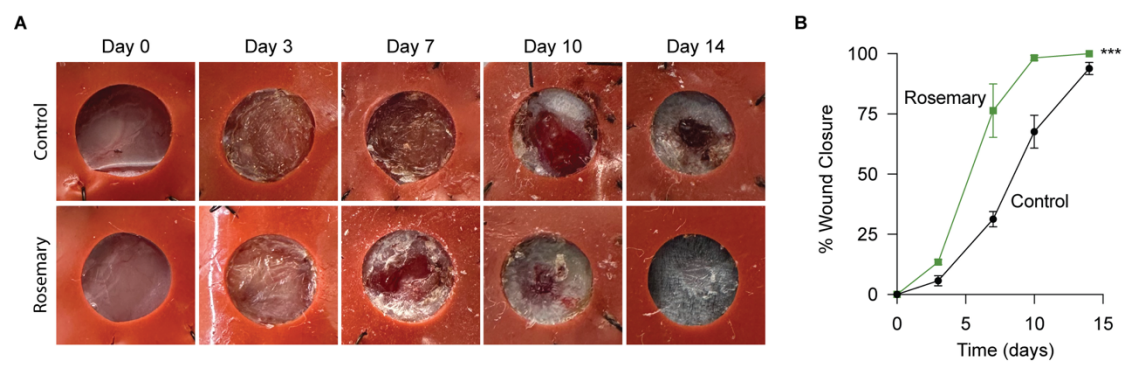


Figure 2: Topical rosemary cream promotes cutaneous mouse back wound closure.

(A) Representative photographs of vehicle control cream- and rosemary cream-treated stented dorsal back wounds on WT mice. Stent hole diameter is 6 mm. (B) Percentage of wound closure in vehicle control cream- (solid black line, n=5) and rosemary cream-treated (solid green line, n=4) WT mouse dorsal stented back wounds. Two-way ANOVA. Data are presented as mean \pm SEM. *P<0.05, **P<0.01, ***P<0.001, ****P<0.0001.

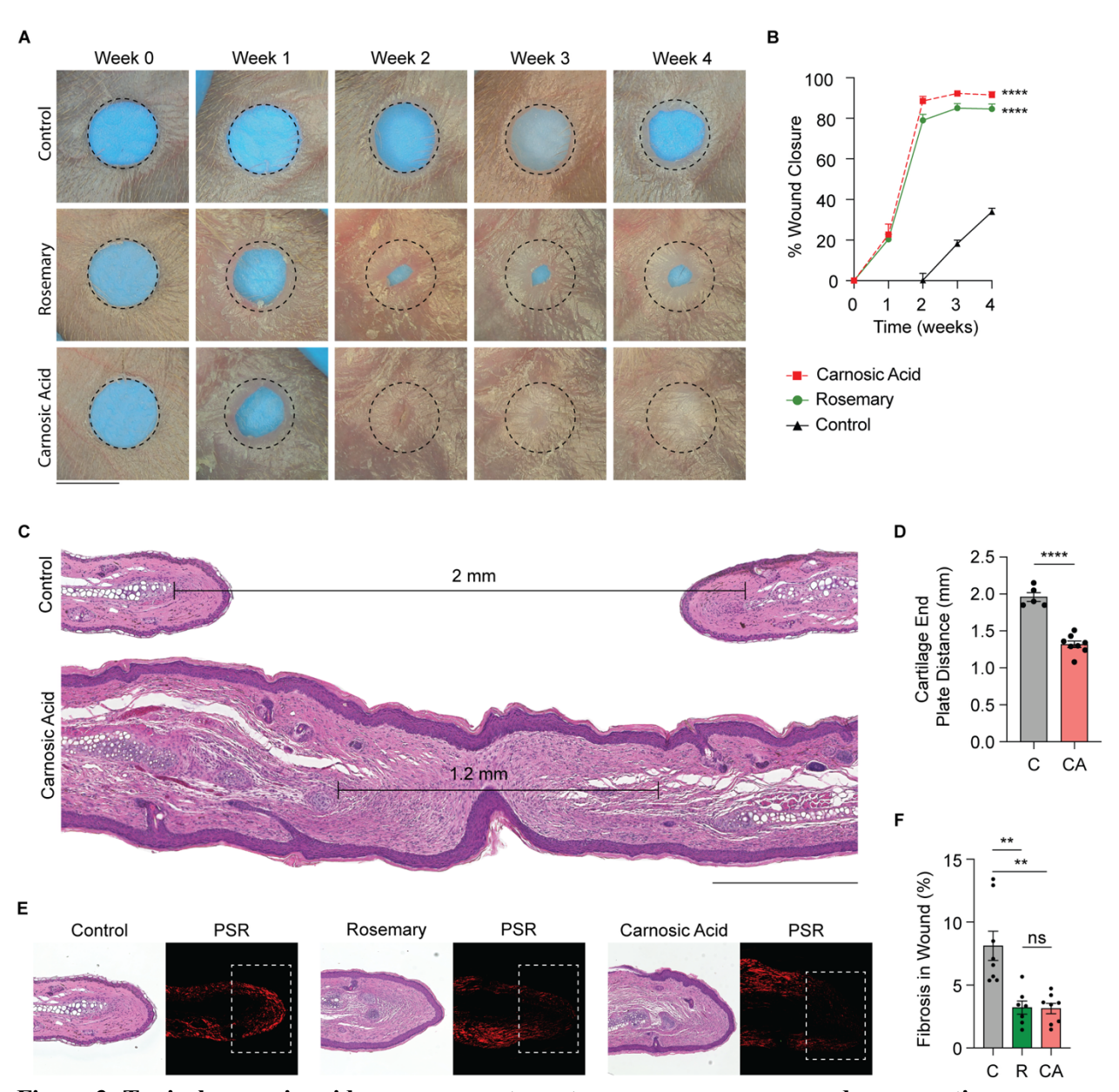


Figure 3: Topical carnosic acid cream promotes cutaneous mouse ear wound regeneration.

(A) Representative photographs of vehicle control cream-, rosemary cream-, or carnosic acid cream-treated WT ears. Dotted circle represents original 2mm hole-punch size. Black scale bar represents 2 mm. (B) Percentage of wound closure in vehicle control cream- (solid black line, n=12), rosemary cream-treated (solid green line, n=12), or canosic acid cream-treated (dotted red line, n= 14) WT mouse ears. Two-way ANOVA. (C) H&E-stained representative tissue sections from vehicle control cream- and carnosic acid cream-treated WT mouse ears. Distance between opposing cartilage endplates are marked. Black scale bar represents 0.5 cm. (D) Bar plot quantifying cartilage endplate distance in between control-and carnosic acid cream-treated WT mouse ears (C = control, CA = carnosic acid). Student's t-test two tailed and unpaired. (E) Representative H&E-stained or PSR-stained images of WT mouse ears treated with vehicle control cream, rosemary cream, or carnosic acid cream. (F) Bar plot quantifying fibrosis by picrosirius red stain at the wound edge tissue from vehicle control cream-, rosemary cream-, or canosic acid cream-treated WT mouse ears (C = control, R = rosemary, CA = carnosic acid). Student's t-test two tailed and unpaired. Data are presented as mean ± SEM. *P<0.05, **P<0.01, ***P<0.001, ****P<0.001.

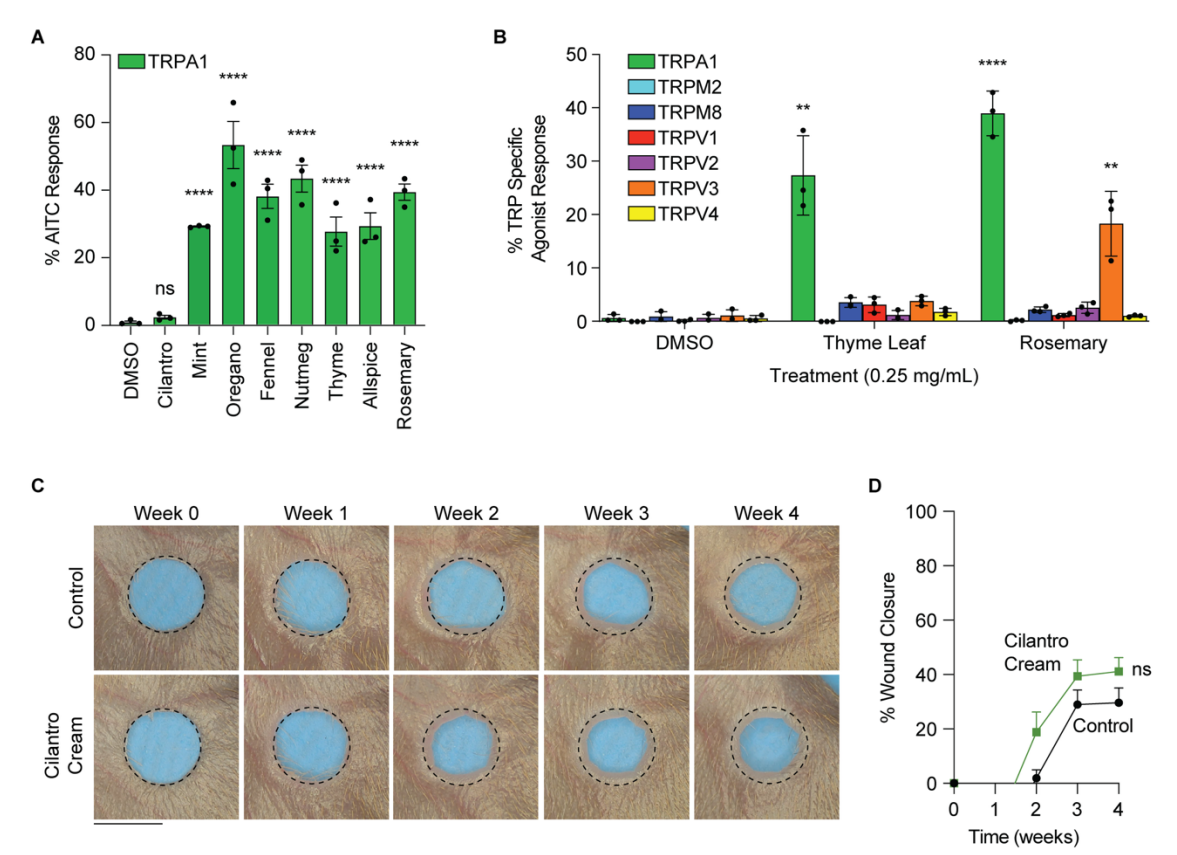


Figure 4: Rosemary extract activates the TRPA1 nociceptor.

(A) Calcium flux assay responses of TRPA1 over-expressing HEK cells treated with different extracts reported as a percent of a TRPA1 specific agonist. One-way ANOVA. (B) Calcium flux assay responses of HEK cells stably over expressing different TRP ion channels treated with rosemary or thyme extract reported as percent of each TRP channel's specific agonist. Student's t-test two tailed and unpaired between DSMO response and thyme or rosemary response. (C) Representative photographs of vehicle control cream- or cilantro cream-treated WT ears. Dotted circle represents original 2mm hole-punch size. Black scale bar represents 2 mm. (D) Percentage of wound closure in vehicle control cream- (solid black line, n=6) or cilantro cream-treated (solid green line, n=7) WT mouse ears. Two-way ANOVA. Data are presented as mean \pm SEM. *P<0.05, **P<0.01, ***P<0.001, ****P<0.0001.

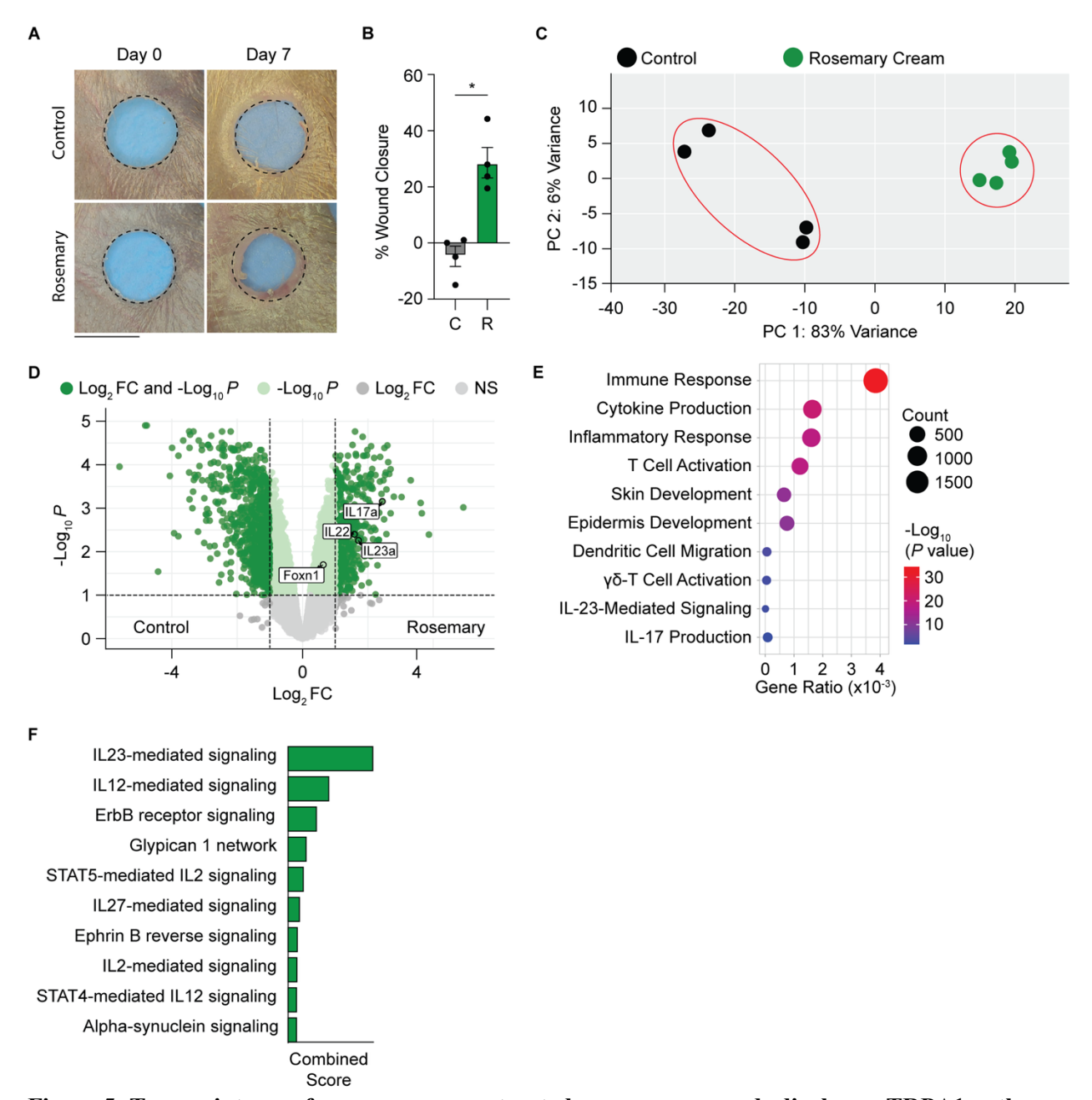


Figure 5: Transcriptome of rosemary-cream treated mouse ear wounds displays a TRPA1 pathway activation profile.

(A) Representative photographs of vehicle control cream- or rosemary cream-treated WT ears at day 7 after injury. Dotted circle represents original 2mm hole-punch size. Black scale bar represents 2 mm. (B) Percentage of wound closure at day 7 in vehicle control cream- (C, n=4) or rosemary cream-treated (R, n=4) WT mouse ears. Student's t-test two tailed and unpaired. *P<0.05 (C) Principal component analysis of vehicle control cream- (black dots) or rosemary cream- (green dots) treated WT ears. (D) Volcano plot of all differentially expressed genes in WT mouse ears treated with vehicle control cream or rosemary cream. (E) Gene ontology analysis of biological processes significantly upregulated in rosemary cream-treated WT mouse ears. (F) Enrichr pathway analysis of WT mouse ears treated with rosemary cream. Combined score is computed by taking the log of the p-value from the Fisher exact test and multiplying that by the z-score of the deviation from the expected rank. Data are presented as mean ± SEM.

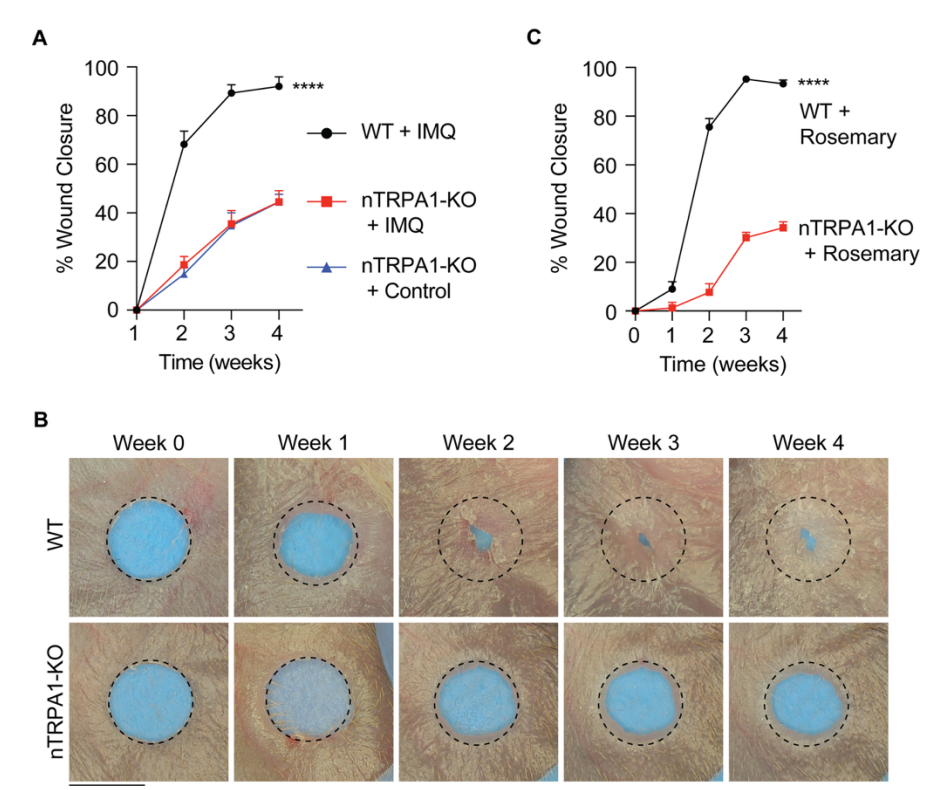


Figure 6: TRPA1 on cutaneous sensory neurons is necessary for rosemary cream mediated ear wound regeneration.

(A) Percentage of ear wound closure of WT littermate control mice treated with IMQ cream (solid black line, n=6), or nTRPA1-KO mice treated with vehicle control cream (solid blue line, n=3) or IMQ cream (solid red line, n=5). Two-way ANOVA of WT + IMQ vs nTRPA1-KO + IMQ. (B) Representative photographs of rosemary cream-treated WT mouse ears or nTRPA1-KO mouse ears. Dotted circle represents original 2mm hole-punch size. Black scale bar represents 2 mm. (C) Percentage of ear wound closure of WT control mice treated with rosemary (solid black line, n=8), or nTRPA1-KO mice treated with rosemary cream (solid red line, n=12). Two-way ANOVA. Data are presented as mean ± SEM. *P<0.05, **P<0.01, ***P<0.001, ****P<0.0001.

Table 1. Full chemical composition of ethanol-based rosemary extract Total area (% Compounds Mass $[M - H]^{-}(m/z)$ RT (min) Abundance) 12.20 Carnosic acid 331.216 8.61 5.29 Carnosol 329.199 7.61 3.13 Rosmarinic acid 359.109 3.46 1.60 Ursolic acid 455.416 10.47 1.51 Quinic acid 191.017 0.298 1.31 12-methoxy-carnosic acid 9.20 345.242 1.28 301.197 Hespertin 8.37 1.19 Methyl rosmarinate 373.234 8.18 1.00 Carnosol isomer 329.201 7.82 1.00 Gallocatechin 305.083 2.04 Rosmaridiphenol 0.86 315.208 8.19 0.82 Pectolinarigenin 313.082 4.89 Pectolinarigenin isomer 0.70 313.085 5.48 Micromeric acid 0.66 453.402 9.87